European Journal of Medical Research

RESEARCH

Open Access

SIRT1/PGC-1α-mediated mitophagy participates the improvement roles of BMAL1 in podocytes injury in diabetic nephropathy: evidences from in vitro experiments

Yanxia Rui[1†], Yinfeng Guo[1†], Linying He[2], Min-er Wang[2] and Henglan Wu[1,3*]

Abstract

Background Dysfunction in podocyte mitophagy has been identified as a contributing factor to the onset and progression of diabetic nephropathy (DN), and BMAL1 plays an important role in the regulation of mitophagy. Thus, this study intended to examine the impact of BMAL1 on podocyte mitophagy in DN and elucidate its underlying mechanisms.

Materials and methods High D-glucose (HG)-treated MPC5 cells was used as a podocyte injury model for investigating the potential roles of BMAL1 in DN. Mitophagy was examined by detecting autophagosomes using transmission electron microscopy, and detecting the colocalization of LC3 and Tom20 using immunofluorescence staining. The interaction between BMAL1 and SIRT1 was conducted by immunoprecipitation (Co-IP) assay.

Results In HG-induced podocyte injury model, we found that BMAL1 and SIRT1 mRNA level was significantly decreased, and positively correlated with mitophagy dysfunction. BMAL1 overexpression could ameliorate HG-induced podocyte injury, evidenced by improved cell viability, decreased cell apoptosis and inflammatory cytokines expression (TNF-α, IL-1β, and IL-6). BMAL1 overexpression could promote podocyte mitophagy coupled with increased expression of mitophagy markers PINK1 and Parkin. In terms of mechanism, Co-IP suggested that BMAL1 could interact with SIRT1. SIRT1 inhibitor Ex-527 addition obviously inhibit the effect of BMAL1 overexpression on the mitophagy, demonstrating that BMAL1 may act on mitophagy by SIRT1//PGC-1α axis.

Conclusions Our in vitro experiments demonstrate that BMAL1/SIRT1/PGC-1α pathway may protect podocytes against HG-induced DN through promoting mitophagy.

Keywords BMAL1, Mitophagy, SIRT1/PGC-1α, Diabetic nephropathy, Podocyte injury

[†]Yanxia Rui and Yinfeng Guo have contributed equally to the work.

*Correspondence:
Henglan Wu
00136158@zjxu.edu.cn
Full list of author information is available at the end of the article

Introduction

Diabetic nephropathy (DN) represents a prevalent microvascular complication among individuals diagnosed with diabetes, with its prevalence on the rise globally [1]. DN is characterized by thickened basement membranes, glomerular sclerosis and mesangial expansion, leading to decline of glomerular filtration rate [2]. Hyperglycemia, advanced glycation end products and oxidative stress are recognized as primary contributing factors [3, 4]. Nowadays, aside from glucose regulation, dialysis, and kidney transplantation, there are no effective treatments available for DN [5]. Owning to high morbidity and mortality rates of DN, it is urgent to develop effective and innovative therapeutic strategies for patients suffering from DN. Podocytes play a crucial role in capillary filtration within renal tubules, and their loss or dysfunction is closely associated with the advancement of DN [6].

Podocytes are specialized cells with critical roles in regulating the actin cytoskeleton, maintaining the integrity of the filtration barrier, and contributing to the regulation of the extracellular matrix in the kidney. Dysfunction of podocytes can lead to kidney diseases characterized by proteinuria and impaired filtration function, including DN [7, 8]. Notably, owning to difficulty of proliferation, podocytes are demonstrated to rely on mitophagy, a highly conserved autophagy process that selectively clear injured or redundant mitochondria, to preserve their normal structure and functionality [9]. As pivotal intracellular organelle, mitochondria is responsible for controlling energy metabolism, overseeing the production of cellular adenosine triphosphate (ATP) and maintain cell homeostasis, especially in energy-demanding tissues, such as kidney [10]. Beyond serving as energy generators, mitochondria also regulate a multitude of intracellular functions, such as cell proliferation and apoptosis [11]. Mitophagy plays a vital role in ensuring adequate energy provision within cells [12]. In addition, recent studies have demonstrated mitophagy played a role in maintain diabetic condition balance. In addition, suppression of mitophagy in podocytes results in renal dysfunction in individuals with diabetes [13].

Some studies have also showed that the circadian gene BMAL1 has a significant influence on renal physiological functions [14]. Deletion of BMAL1 in renal collecting duct led to elevated urine volume and lowered blood pressure [15]. Meanwhile, lack of BMAL1 cause dysfunction in renal mitochondria and disrupt normal pharmacokinetics, as stated in reference [16]. SIRT1, a member of the class III HDAC family, plays a crucial role in overseeing cellular survival, metabolism, response to oxidative stress, generation of mitochondria, and inflammatory processes [17]. Furthermore, SIRT1 has the ability to boost mitochondrial biogenesis through the activation of peroxisome proliferator-activated receptor gamma coactivator 1 alpha (PGC-1α), an essential controller of mitochondrial generation [18]. Numerous studies have highlighted the close interplay between SIRT1 and BMAL1. For instance, in a myocardial ischemic/reperfusion (IR) model, SIRT1 mitigates injury through cross-talk with BMAL1 [19]. Besides, BMAL1 was reported to improve myocardial injury and inhibit inflammatory activities in the rat model of sepsis though facilitating mitophagy via SIRT1 [20]. Similarly, BMAL1 has been shown to regulate the innate immune system by interacting with SIRT1 in cartilage [21]. However, the exact connection between BMAL1 and SIRT1 in DN remains elusive. Hence, our investigation primarily focuses on the impact of BMAL1 on DN in vitro and subsequently delves into its potential mechanism in podocyte mitophagy.

Materials and methods

Cell culture and treatments

The mouse podocyte cell lines (MPC5) were purchased by Wuhan Shain Biology co. LTD. MPC5 were cultured in a 5% CO_2 incubator at 37 ℃ using RPMI1640 medium containing 10% fetal bovine serum and 10 U/mL interferon gamma (IFN-γ). When cell confluence reached about 80%, cells were digested by pancreatic enzymes. Following differentiation induction, cells were incubated in RPMI 1640 complete medium devoid of IFN-γ at 37℃ and 5% CO_2 for a period ranging from 7 to 14 days. Subsequently, the differentiated podocytes were segregated into two distinct groups: the control and high glucose (HG) group. Within the control group, MPC5 were nurtured in the presence of normal D-glucose (5.5 mmol/L). Conversely, in the HG group, cells were subjected to elevated glucose concentrations (30 mmol/L) for a duration of 24 h to simulate podocyte damage akin to DN [22]. In addition, some cells would be treated with EX-527 (SIRT1 inhibitor, 10 mmol/L) or FCCP (mitophagy agonist, 10 μM) for 24-h culture.

Cell transfection

Lentivirus vectors system from VectorBuilder (Guangzhou, China) was used to overexpress BMAL1 in MPC5 cells. The oe-BMAL1 sequence was acquired from the NCBI website. Lentivirus vectors that interfered with BMAL1 were constructed and were transfected into MPC5 using HighGene reagent together with packaging plasmid. After 48 h for transfecting, lentivirus particles were collected and concentrated. For lentivirus infections, MPC5 were collected and then planted in 6-well plates (2×10^5 cells/well), then the virus (1×10^8 TU/mL) was transfected into MPC5. After 48 h of lentivirus infections, stable transfected cells were selected by adding

2.5 g/mL puromycin. The cells were divided into: (i) HG (30 mmol/L) + Vector; (ii) HG (30 mmol/L) + oe-BMAL1; (iii) HG (30 mmol/L) + oe-BMAL1 + EX-527 (Ex, a SirT1 inhibitor, 10 mmol/L); (iv) HG (30 mmol/L) + oe-BMAL1 + Ex (10 mmol/L) + FCCP (10 μM).

CCK-8 assay

CCK-8 colorimetric method was used to measure cell proliferation. MPC5 and BMAL1-overexpressed MPC5 were seeded into 96-well plates (100 μL/well) with condition of 5% CO_2 at 37 ℃ for cell adhesion growth. After adding 10 μL of CCK-8, cells in each well were then underwent for an additional 2 h in darkness. Subsequently, the absorbance of each well was measured at 450 nm using a microplate reader (Wuxi Hiwell Diatek, DR-3518G).

Cell apoptosis assay

Cell apoptosis was assessed utilizing an Annexin V-FITC/PI apoptosis detection kit (Beyotime, China) as per the manufacturer's instructions. Following 24 h of cell culture, cells from each group were detached using 0.25% pancreatic enzyme without EDTA and collected via centrifugation at 1500 rpm for 5 min. Following this, the cells were rinsed twice and suspended in 300 μL of binding buffer. Subsequently, cells were labeled with 5 μL of fluorescein isothiocyanate (FITC) annexin V for 5 min, followed by a 15-min incubation with 10 μL of propidium iodide (PI). Subsequently, apoptosis levels were analyzed via flow cytometry, and the results were interpreted using CELL Quest software.

RNA extraction and qRT-PCR

BMAL1 and SIRT1 expression levels were determined using qRT-PCR following manufacturer's instructions for the standard SYBR Green PCR kit (Lifeint, China). Initially, cellular RNA was isolated using the TRIzol reagent (Invitrogen, Carlsbad, CA), followed by the synthesis of cDNA from the reverse-transcribed RNA using the PrimeScript RT Reagent Kit (Takara, Japan). Expression of each gene was quantified using comparative threshold cycle method with GAPDH as an internal reference. All assays were run in triplicate as follows: step 1: denaturation at 95 °C for 3 min; step 2: 40 cycles of 95 °C for 12 s and 62 °C for 40 s. The qRT-PCR process was conducted in accordance with the reported methods [23]. The primer sequences applied were as follows: BMAL1, 5′-AATGAGCCAGACAACGAGGG-3′ (forward primer) and 5′-GCTGTCGCCCTCTGATCTAC-3′ (reverse); SIRT1, 5′-CGGCTACCGAGGTCCATATAC-3′ (forward primer) and 5′-CTGCAACCTGCTCCA AGGTA-3′ (reverse); PGC-1α, 5′-GGTACCCAAGGC AGCCACT-3′ (forward primer) and 5′-GTGTCCTCG GCTGAGCACT-3′ (reverse); GAPDH, 5′-TGTGAA CGGATTTGGCCGTA-3′ (forward primer) and 5′-CAA TCTCCACTTTGCCACTGC-3′ (reverse).

Western blotting assay

Expression of BMAL1, SIRT1, PGC-1α, PINK1, and Parkin in cells was also detected by Western blotting assay. Total protein from and cells were quantified by a bicinchoninic acid assay. Following the collection of total cellular protein, cell lysates were prepared by 100 μL of RIPA lysis buffer. Protein samples (25 μg loading protein per well) were subsequently separated by 12% SDS–PAGE and transferred onto polyvinylidene fluoride (PVDF) membranes through electrophoresis. Following this, membranes were blocked with 5% skim milk for 1 h and then exposed to the primary antibodies: anti-BMAL1 (1: 1,0000, ab93806, Abcam, UK), anti-SIRT1 (1: 1,0000, 9475, CST, US), anti-PGC-1α (1: 10,000, 9475, CST, US), anti-PINK1 (1: 1,0000, ab216144, Abcam, UK) and anti-Parkin (1: 10,000, 2132, CST, US) overnight at 4 °C. Next, membranes were rinsed with TBST buffer and then exposed to secondary HRP-conjugated goat anti-rabbit IgG antibody (1:2,000, ab6721, Abcam, UK) for 1 h at 37 °C. The signals were detected by an electrochemiluminescence reagent (Applygen Co., Ltd. Beijing, China), and the bands were visualized through autoradiography.

ELISA assay

Inflammatory cytokine levels, including Tumor Necrosis Factor-α (TNF-α), Interleukin-1β (IL-1β), and Interleukin-6 (IL-6) levels were quantified using commercial ELISA kits (Beyotime, Shanghai, China) following the provided protocols.

Co-immunoprecipitation (Co-IP) assays

Co-IP assays were performed to detect the interaction between BMAL1 and SIRT1. When cell confluence reached over 90%, the cells were harvested by scraping. The supernatant was collected by centrifugation, and then incubated with primary antibodies (anti-BMAL1 and anti-SIRT1) or isotype immunoglobulin G (IgG), gentle rocking 2 h at 4 °C. Following this, protein A/G beads were added to the immunoprecipitation mixture and gently rocked overnight at 4 °C. The following day, the mixtures were washed with Elution buffer, and the resulting supernatants were collected for subsequent Western blot analysis.

ATP assay

ATP levels were assessed following protocol of an ATP Assay Kit (Solarbio, Beijing, China). Cells were harvested and mixed with an ATP detection reagent. The chemiluminescence intensities of samples and standards were

then measured using an Ultraviolet spectrophotometer. ATP levels were quantified by referencing the standard curve and were subsequently normalized to the protein content.

Determination of reactive oxygen species (ROS) production

Intracellular ROS levels were measured with the DCFH-DA fluorescence probe per the manufacturer's instructions (cat. no. S0033M; Beyotime Biotechnology). Treated MPC5 were collected, rinsed twice with PBS, and then exposed to DCFH-DA (10 μM) for 20 min in darkness at 37 °C. Following incubation, the average intensity of ROS was determined by flow cytometry, and data analysis was conducted using FlowJo software.

Measurement of mitochondrial membrane potential (MMP)

The MMP was evaluated using the JC-1 dye kit (C2006, Beyotime, Shanghai, China) as per the manufacturer's guidelines. In summary, MPC5 cells were harvested, rinsed twice with PBS, and subsequently exposed to JC-1 for 20 min at 37 °C in a light-protected environment. Subsequently, the data were analyzed and averaged using flow cytometry, with further analysis performed using FlowJo software.

Transmission electron microscope (TEM)

Cells were fixed using 2.5% glutaraldehyde for 48 h, and then were secondarily fixed with1% osmium tetroxide for 2 h at 4 ℃. After washing, cell samples were dehydrated and embedded in acetone–EPON812 embedding agent (1:1 volume ratio). Ultrathin sections were prepared using an ultramicrotome, then stained with 2% uranyl acetate and lead citrate. Subsequently, the samples were examined by Tecnai 30 transmission electron microscope to identify autophagosomes within the podocytes. Each sample underwent careful scrutiny, and podocytes were randomly selected for quantifying the number of autophagosomes and autophagolysosomes.

Immunofluorescence

Cells were adhered to coverslips and then exposed to primary antibodies, including anti-Tom20 (1:200, ab56783, Abcam) and rabbit anti-LC3 (1:200, ab192890, Abcam), overnight at 4 °C. Subsequently, the slides were incubated with fluorescein isothiocyanate or tetramethyl rhodamine isothiocyanate-conjugated secondary antibodies for 45 min and stained with 6-diamidino-2-phenylindole (DAPI, Beyotime). Finally, examination was conducted using a confocal fluorescence microscope (Leica, Germany).

Statistical analysis

The statistical analysis was performed using GraphPad 8.0 software. The results were expressed as mean ± standard deviation. Student's *t* test was utilized to evaluate the statistical significance of variances between two treatment groups, and analysis of variance (ANOVA) followed Tukey's multiple comparison for three or more groups. $P < 0.05$ indicates statistical significance.

Results

HG decreased the podocytes cell viability and promoted apoptosis

To examine HG effect on the podocytes, CCK8 and flow cytometry were conducted to examine the cell viability and apoptosis. Results showed that, compared with control cells, cell viability in HG group decreased after 24 h co-incubation ($P < 0.01$, Fig. 1A), and HG promoted cell apoptosis ($P < 0.01$, Fig. 1B).

The BMAL1/SIRT1/PGC-1α pathways and mitophagy damage are inhibited in HG induced podocytes injury

To examine whether BMAL1 and SIRT1/PGC-1α pathways are involved in HG-induced DN, levels of these factors in MPC5 (control) and HG-treated MPC5 (HG group) were determined by qRT-PCR and western blotting. Both mRNA and protein levels of BMAL1 and SIRT1 in the HG group were considerably lower than the control group, while the PGC-1α was increased ($P < 0.01$, Fig. 1C, D). Meanwhile, mitophagy markers (PINK1 and Parkin) expression was decreased with increased inflammatory cytokines (TNF-α, IL-1β, and IL-6) expression after HG induction ($P < 0.01$, Fig. 2A, B), indicating that mitophagy damage was deteriorating and inflammation was aggravated. In addition, Co-IP results confirmed the protein association between BMAL1 and SIRT1 in HG induced podocytes (Fig. 2C).

Overexpression BMAL1 improved HG-induced podocytes injury

To explore the influence of BMAL1 on podocyte injury induced by HG, we successfully overexpressed BMAL1 in HG-treated MPC5 cells. As depicted in Fig. 3A, B, both mRNA and protein expression of BMAL1 was higher in HG + oe-BMAL1 group in comparison with that in HG + Vector (control) group. Our qRT-PCR analysis demonstrated a significant increase in SIRT1 levels and a notable reduction in PGC-1α levels in the HG + oe-BMAL1 group compared to the HG + Vector (control) group ($P < 0.01$, Fig. 3A), a finding consistent with our western blot results ($P < 0.01$, Fig. 3B). Furthermore, overexpression of BMAL1 in HG-induced DN led to an enhanced cell viability and reduced cell

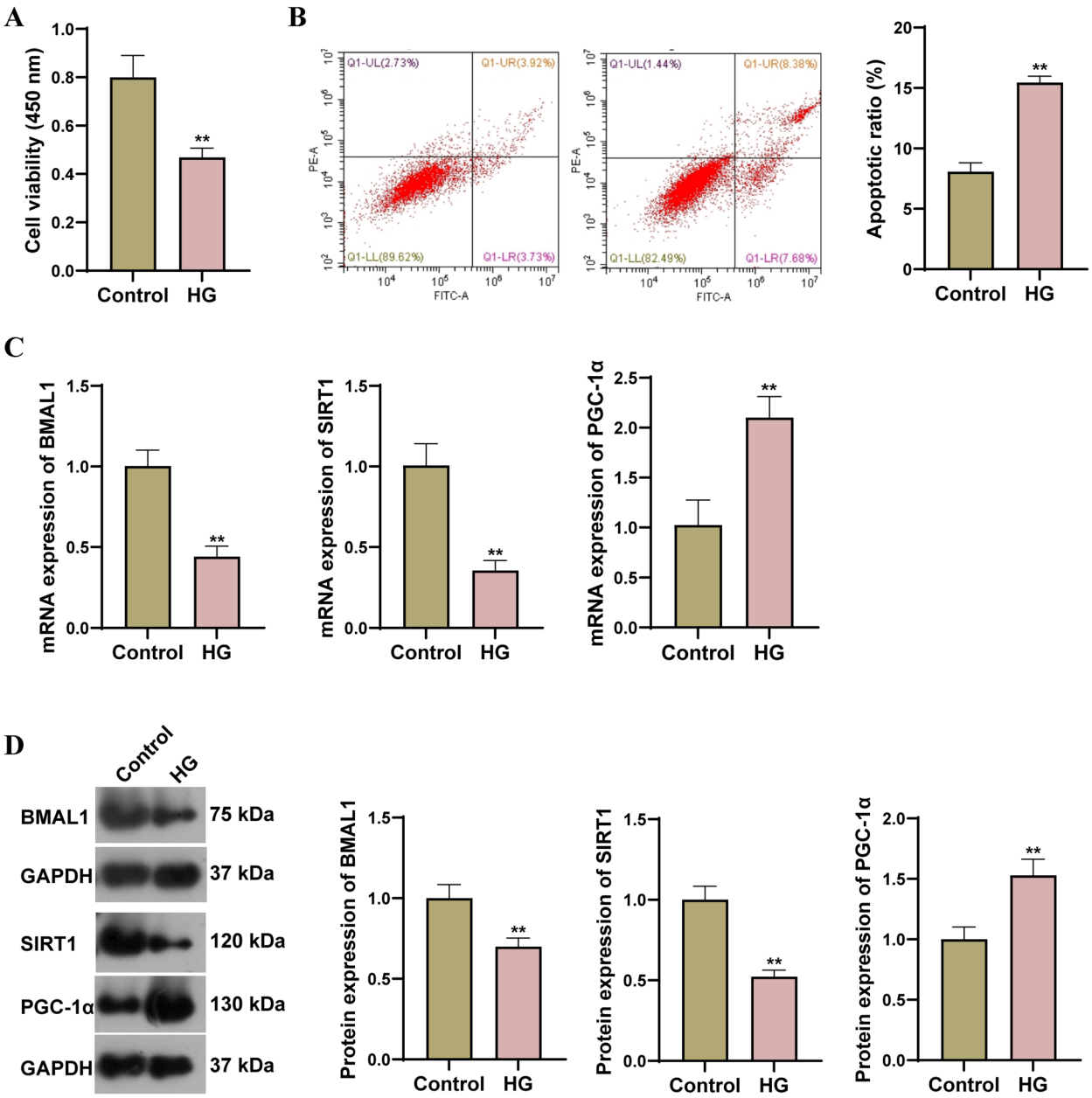

Fig. 1 High-glucose (HG) decreased the podocytes cell viability and promoted apoptosis. **A** Cell viability of podocytes in MPC5 (normal) and HG-treated MPC5 (30 mmol/L HG) analyzed by CCK-8; **B** apoptosis of podocytes in MPC5 (normal) and HG-treated MPC5 (30 mmol/L HG) groups analyzed by flow cytometry; **C**, **D** mRNA expression of BMAL1, SIRT1 and PGC-1α (**C**), protein expression of BMAL1, SIRT1 and PGC-1α (**D**) in MPC5 (normal) and HG-treated MPC5 (30 mmol/L HG) groups. $N = 3$ in each group, $^{**}P < 0.01$ vs control

apoptosis compared to the HG + Vector (control) group ($P < 0.01$, Fig. 3C, D). Moreover, we found that BMAL1 overexpression resulted in decreased levels of TNF-α, IL-1β, and IL-6, alongside an increase in mitophagy in the HG + oe-BMAL1 group compared to the HG + Vector (control) group ($P < 0.01$, Fig. 3E, F). Taken together, we verified that BMAL1 overexpression played role in improving HG-induced podocytes injury, probably by regulating SIRT1/PGC-1α axis.

BMAL1 overexpression improved HG-induced podocyte injury by promoting SIRT1/PGC-1α-mediated mitophagy

To demonstrate the improvement roles of BMAL1 in podocyte injury was achieved by targeting SIRT1/

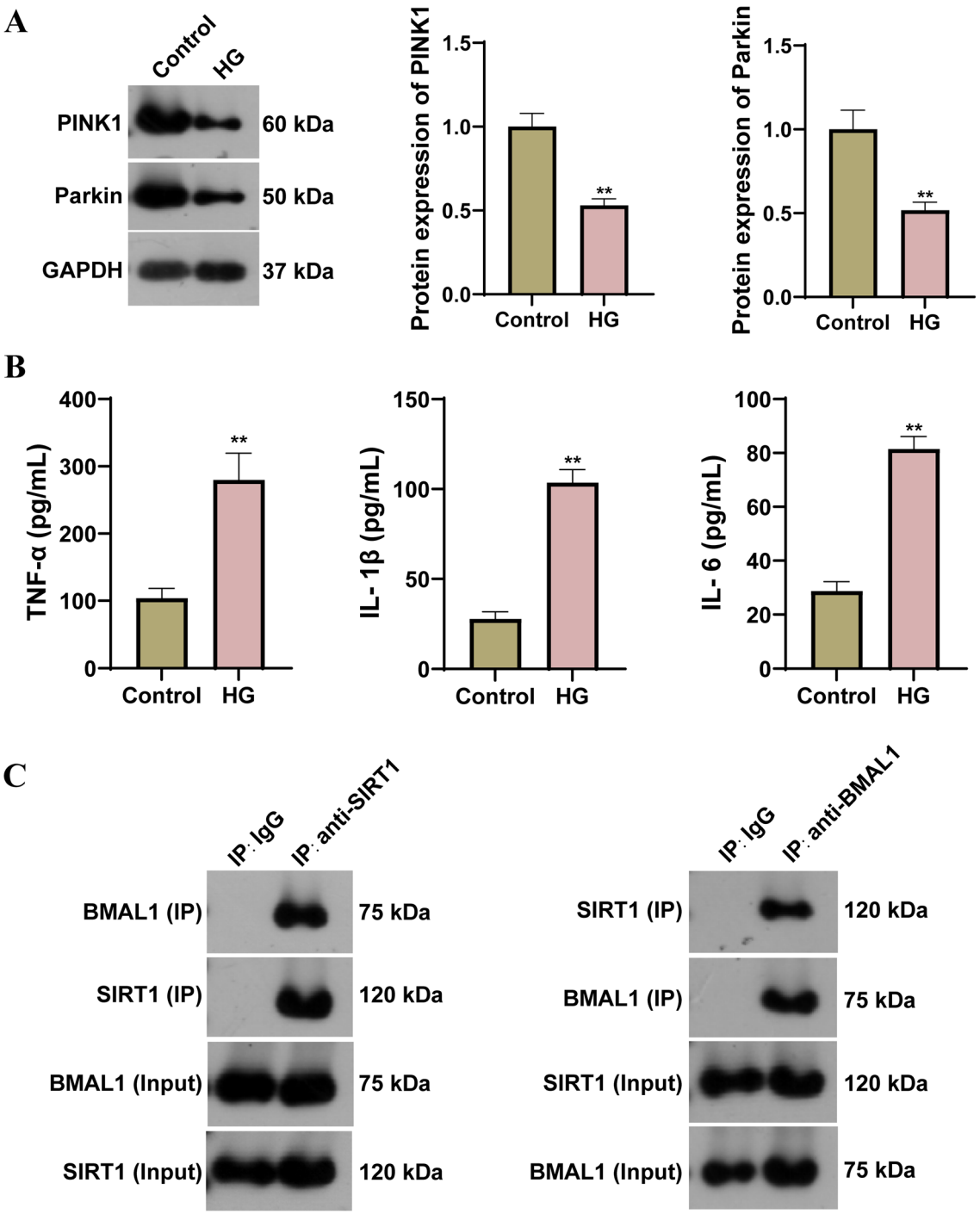

Fig. 2 Mitophagy damage was inhibited and in high-glucose-induced podocytes. **A** Expression of PINK1 and Parkin in MPC5 (normal) and HG-treated MPC5 (30 mmol/L HG) analyzed by western blotting; **B** Levels of TNF-α, IL-1β, and IL-6 in MPC5 (normal) and HG-treated MPC5 (30 mmol/L HG) detected by ELISA. $N=3$ in each group, $^{**}P<0.01$ vs Control. **C** CO-IP detection of the interaction between BMAL1 and SIRT1

PGC-1α-mediated mitophagy, we used EX-527 (Ex, a SirT1 inhibitor, 10 mmol/L) to repress SIRT1, and used FCCP (mitophagy agonist) to activate mitophagy. Figure 4A illustrates that BMAL1 overexpression could upregulated level of PINK1 and Parkin compared to corresponding vector group ($P<0.01$, Fig. 4A). In addition, Ex-527 addition obviously inhibit the effect of BMAL1 overexpression on the mitophagy with the lower level of

PINK1 and Parkin in the HG-induced podocyte injury ($P < 0.01$, Fig. 4A). However, FCCP addition reverse the effect of Ex-527 on the mitophagy. Furthermore, levels of ATP and MMP were obviously higher, while level of ROS was markedly lower after BMAL1 overexpression than that in vector group, and Ex-527 addition obviously reversed such changes on the ATP, MMP and ROS levels ($P < 0.01$, Fig. 4B–D). Besides, these results, including PINK1 and Parkin expression as well as the levels of ATP, MMP and ROS resulted from EX-527 treatment (SIRT1 inhibition) were restored by FCCP treatment (mitophagy activation). All the outcomes revealed that BMAL1 overexpression improved HG-induced podocyte injury by promoting mitophagy via SIRT1/PGC-1α pathway.

Subsequently, mitochondrial autophagosomes were observed by means of TEM (Fig. 5A). There were increased number of mitochondrial autophagosomes in HG + oe-BMAL1 group, while such changes were reversed after adding Ex-527. In comparison with HG + oe-BMAL1 + Ex group, number of mitochondrial autophagosomes were further increased after adding FCCP (Fig. 5A). By employing dual immunofluorescence staining with LC3-II and Tom20, we visualized the labeling of autophagosomes and mitochondria, respectively. This approach allowed us to observe a substantial increase in LC3-positive autophagosome formation within cells of the HG + oe-BMAL1 group, demonstrating co-localization with mitochondria compared to the HG + oe-BMAL1 + Ex group. Notably, this effect was reversed by FCCP (Fig. 5B). In summary, BMAL1 overexpression significantly ameliorated mitochondrial dysfunction and reduced apoptosis stimulated by HG through SIRT1/PGC-1α-mediated mitophagy.

Discussion

DN is typically identified as a condition affecting podocytes, characterized by the infiltration of immune cells and persistent inflammation. This leads to the progressive deterioration of renal function, ultimately culminating in renal failure [24]. Disrupted mitophagy significantly contributes to the development of DN. Our research demonstrated that elevating BMAL1 levels increased podocyte proliferation, inhibited cell apoptosis, and enhanced mitophagy in DN induced by HG. We found that SIRT1 downregulates the transcriptional level of PGC-1α, and BMAL1 overexpression upregulated SIRT1, thereby improving podocyte mitophagy injury. This study is the first to elucidate the mechanism of BMAL1/SIRT1/PGC-1α-mediated mitophagy abnormalities in podocyte injury in DN. Our findings indicate that BMAL1 plays a role in mitochondrial biogenesis and mitochondria-mediated apoptosis in DN, and it regulates PGC-1α by modulating SIRT1. Hence, this study suggests that BMAL1 may protect podocytes against HG-induced DN by promoting SIRT1/PGC-1α-mediated mitophagy.

Mitochondrial biogenesis is a crucial biological process that enhances mitochondrial quantity and ATP production [25]. Mitophagy serves to prevent the excessive accumulation of ROS and triggers the mitochondrial apoptotic cascade, thereby mitigating kidney injury [26]. Podocytes, as highly differentiated postmitotic cells, exhibit limited regeneration capabilities, making their fate heavily reliant on their ability to respond to stimuli [27]. Podocyte mitophagy dysfunction was identified as a key factor driving the advancement of DN [27]. This study found that upregulated level of BMAL1 enhanced mitophagy of podocyte exposed to high glucose via regulating mitophagy-related proteins. As the primary transcriptional activator of the circadian clock, BMAL1 plays a pivotal role in regulating the progression of renal diseases [28]. Earlier research has shown that BMAL1 expression declines in cardiac and cerebral tissues following renal ischemia–reperfusion injury (IRI). Furthermore, IRI can diminish SIRT1 activity via diverse signaling pathways [29]. YANG et al. investigated the regulatory connection between BMAL1 and SIRT1. Their findings revealed that BMAL1 depletion resulted in decreased SIRT1 expression, suggesting a direct interaction between endogenous BMAL1 and SIRT1 proteins in human cartilage [21]. In our current investigation, we observed that BMAL1 might modulate SIRT1 expression in DN.

Mitochondrial biogenesis, orchestrated by SIRT1, plays a pivotal role in the progression of diseases [30]. SIRT1 could enhance mitochondrial biogenesis via PGC-1α-dependent pathways [31]. Previous research has established that resveratrol activates AMPK, thereby stimulating SIRT1, which subsequently induces the

(See figure on next page.)

Fig. 3 Overexpression of BMAL1 improved the cell viability of HG induced podocytes and inhibited the cell apoptosis. **A** mRNA expression of BMAL1, SIRT1 and PGC-1α in HG-treated MPC5 transfecting with oe-BMAL1 and vector (control); **B** protein expression of BMAL1, SIRT1 and PGC-1α in HG-treated MPC5 transfecting with oe-BMAL1 and Vector (control); **C**, **D** cell viability and apoptosis (**D**) of HG-treated MPC5 transfecting with oe-BMAL1 and vector (control); **E** ELISA assay reveals the levels of TNF-α, IL-1β, and IL-6 in HG-treated MPC5 transfecting with oe-BMAL1 and Vector (control); **F** protein expression of PINK1 and Parkin in HG-treated MPC5 transfecting with oe-BMAL1 and vector (control). $N = 3$ in each group, $^{**}P < 0.01$ vs control

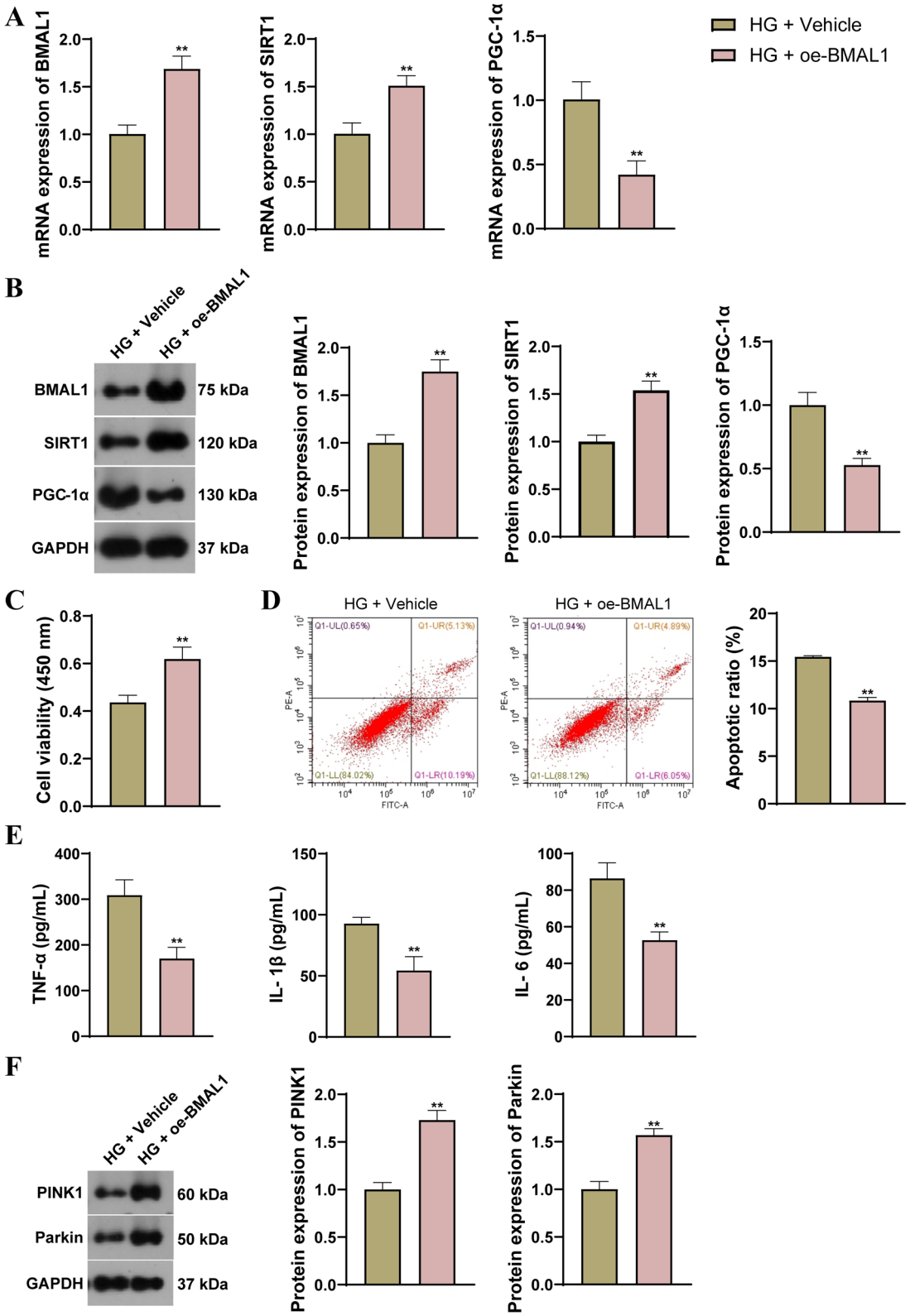

Fig. 3 (See legend on previous page.)

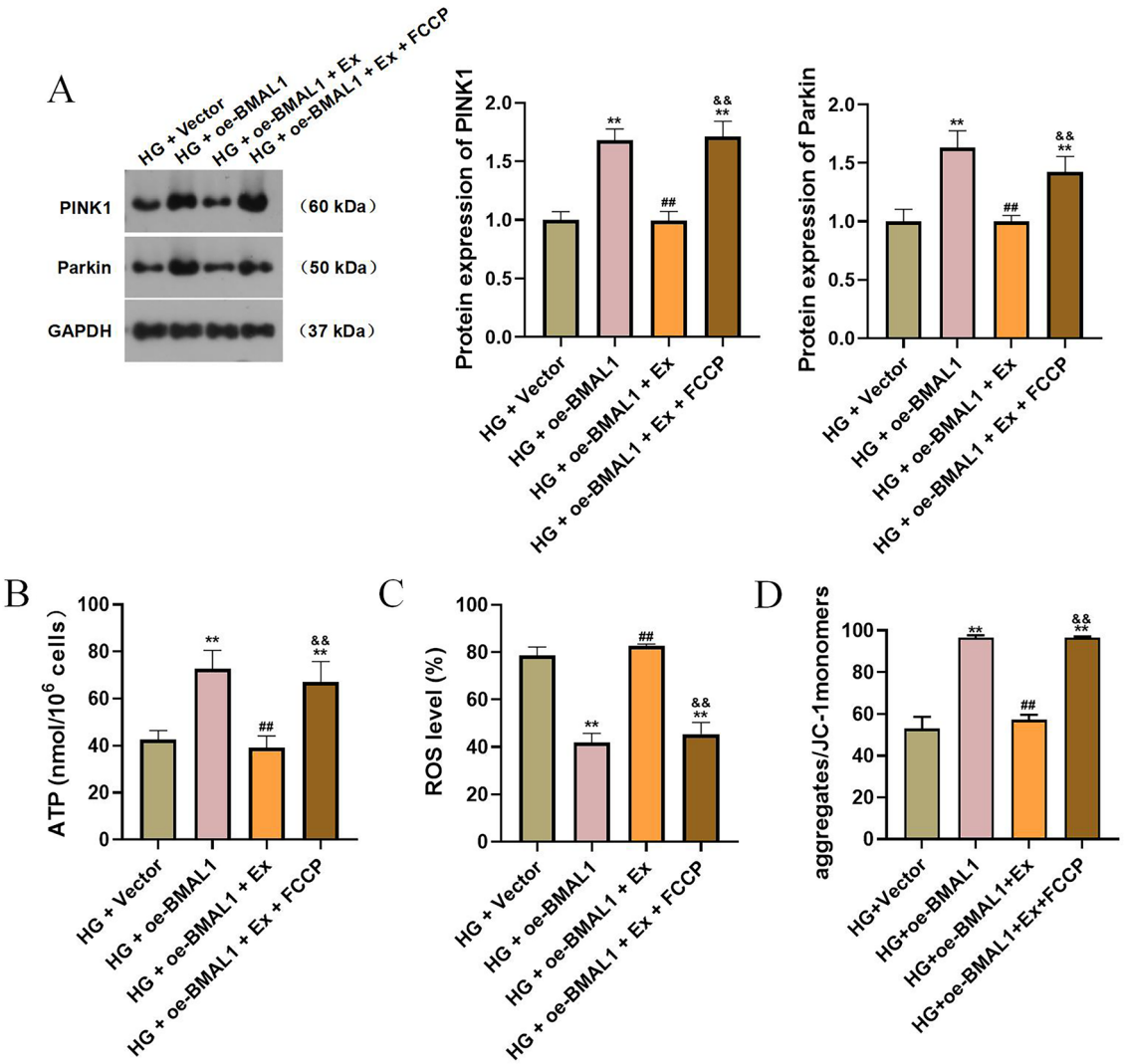

Fig. 4 BMAL1 overexpression improved HG-induced podocyte injury by promoting mitophagy. **A** PINK1 and Parkin expression in each group analyzed by western blotting; **B**–**D** Levels of ATP (**B**), ROS (**C**), and MMP (**D**) in each group detected by assay kits. HG, high glucose; vector, a negative control of oe-BMAL1; Ex, EX-527, an SIRT1 inhibitor; FCCP, mitophagy agonist. $N=3$ in each group. $^{**}P<0.01$ vs control. $^{**}P<0.01$ vs HG + vector; $^{\#\#}P<0.01$ vs HG + oe-BMAL1; $^{\&\&}P<0.01$ vs HG + oe-BMAL1 + Ex

phosphorylation of PGC-1α. This phosphorylation event is essential for initiating mitochondrial biogenesis. [32]. PGC-1α, an essential regulator of mitochondrial biogenesis, boosts mitochondrial protein synthesis and functional mitochondrial renewal by amplifying NRF1 activity [33]. Olmos et al. discovered that SIRT1 deacetylates PGC-1α and FoxO3a under conditions of oxidative stress, thereby governing antioxidant gene expression to safeguard mitochondria from apoptosis (34). In our investigation, we observed a decline in SIRT1 activity due to DN, resulting in reduced PGC-1α-dependent mitochondrial biogenesis. Upon administering an exogenous SIRT1 agonist, SIRT1 activity increased, leading to a resurgence in mitochondrial biogenesis via the PGC-1α-dependent pathway and subsequent mitigation of DN damage. Conversely, the use of exogenous mitophagy agonists produced the opposite effect. Thus, our hypothesis suggests that BMAL1 regulates the expression of SIRT1 by binding to its transcriptional promoter. This regulation indirectly influences the expression of PGC-1α, consequently modulating mitophagy.

In fact, there are some remaining limitations in our research. The current study only investigated the role of BMAL1 in cells, and it remains unclear whether BMAL1 exerts similar actions in animal models. Besides, it still remains unclear whether other pathways and

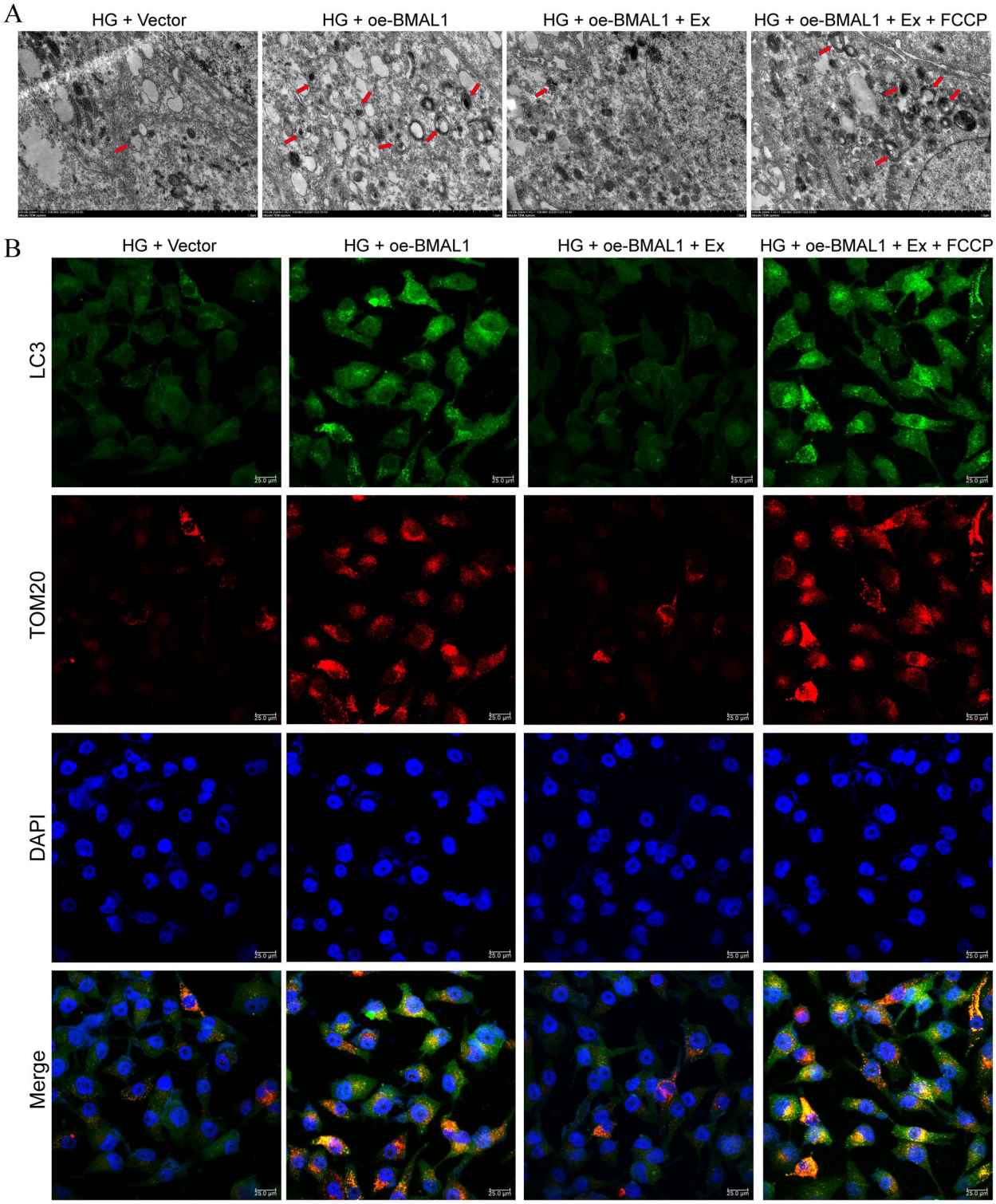

Fig. 5 Observation of mitochondrial autophagosomes. **A** Representative image of mitochondrial autophagosome (1.0 μm); **B** representative image of immunofluorescence double staining of LC3 and Tom20 (25.0 μm). HG, high glucose; vector, a negative control of oe-BMAL1; Ex, EX-527, a SIRT1 inhibitor; FCCP, mitophagy agonist. $N = 3$ in each group

cellular process involved in the role of BMAL1 in podocytes injury in addition to SIRT1/PGC-1α-mediated mitophagy. These should be further explored in future. Most importantly, while results from this study are promising, there is a need of more studies to reveal whether targeting BMAL1 can be used in clinical.

Conclusion

In summary, this study underscores the significance of BMAL1 as a potential therapeutic target in DN, and the roles are achieved partly by regulating mitochondrial homeostasis through the SIRT1/PGC-1α axis. However, this is a preliminary study for exploring the involvements of SIRT1/PGC-1α-mediated mitophagy as an underlying mechanism of BMAL1 in DN, all results were obtained based on in vitro experiments. Further in vivo investigations are needed to confirm the potential of BMAL1 as key targets in DN.

Abbreviations

ATP	Adenosine triphosphate
Co-IP	Co-immunoprecipitation
DN	Diabetic nephropathy
FITC	Fluorescein isothiocyanate
HG	High glucose
IFN-γ	Interferon gamma
IgG	Immunoglobulin G
IL-1β	Interleukin-1β
IL-6	Interleukin-6
IR	Ischemic/reperfusion
IRI	Ischemia–reperfusion injury
MMP	Mitochondrial membrane potential
PGC-1α	Proliferator-activated receptor gamma coactivator 1 alpha
PI	Propidium iodide
ROS	Reactive oxygen species
TNF-α	Tumor Necrosis Factor-α
TEM	Transmission Electron Microscope

Acknowledgements
Not applicable.

Author contributions
Yanxia Rui: Conceptualization, Data curation, Formal analysis, Investigation and Writing-original draft. Yinfeng Guo: Conceptualization, Data curation, Formal analysis, Validation and and Writing-original draft. Lin-ying He: Formal analysis, Investigation, Supervision, and Validation. Min-er Wang: Project administration, Resources, Supervision, and Validation. Henglan Wu: Conceptualization, Data curation, Methodology, Software, Visualization, and Writing-review & editing. All authors read and approved the final manuscript.

Funding
This work was supported by Zhejiang Province Medical and Health Project (grant number 2022KY1235), Zhejiang Province Medical and Health Project (Grant number 2024KY437), and Jiaxing Key Discipline of Medicine–Nephrology (grant number 2023-ZC-011).

Availability of data and materials
The datasets used and/or analysed during the current study are available from the corresponding author on reasonable request.

Declarations

Ethics approval and consent to participate
Not applicable.

Consent for publication
Not applicable.

Competing interests
The authors declare no competing interests.

Author details
[1]Department of Nephrology, Affiliated Hospital of Jiaxing University (The First Hospital of Jiaxing), No.1882, Zhonghuan North Road, Jiaxing 314000, Zhejiang, China. [2]Jiaxing University Master Degree Cultivation Base, Zhejiang Chinese Medical University, Hangzhou 310000, Zhejiang, China. [3]Kidney Disease Center College of Medicine, The First Affiliated Hospital, Zhejiang University, Hangzhou, China.

Received: 19 September 2024 Accepted: 7 January 2025
Published online: 15 January 2025

References

1. Li RY, Guo L. Exercise in diabetic nephropathy: protective effects and molecular mechanism. Int J Mol Sci. 2024;25(7):3605.
2. Rai B, Srivastava J, Saxena P. The functional role of microRNAs and mRNAs in diabetic kidney disease: a review. Curr Diabetes Rev. 2024;20(6): e201023222412.
3. Liu Q, Cui Y, Ding N, Zhou C. Knockdown of circ_0003928 ameliorates high glucose-induced dysfunction of human tubular epithelial cells through the miR-506-3p/HDAC4 pathway in diabetic nephropathy. Eur J Med Res. 2022;27(1):55.
4. Sato S, Takayanagi K, Shimizu T, Kanozawa K, Iwashita T, Hasegawa H. Correlation between albuminuria and interstitial injury marker reductions associated with SGLT2 inhibitor treatment in diabetic patients with renal dysfunction. Eur J Med Res. 2022;27(1):140.
5. Elendu C, John Okah M, Fiemotongha KDJ, Adeyemo BI, Bassey BN, Omeludike EK, et al. Comprehensive advancements in the prevention and treatment of diabetic nephropathy: a narrative review. Medicine. 2023;102(40): e35397.
6. Li X, Zhang Y, Xing X, Li M, Liu Y, Xu A, et al. Podocyte injury of diabetic nephropathy: novel mechanism discovery and therapeutic prospects. Biomed Pharmacother. 2023;168:115670.
7. Audzeyenka I, Bierżyńska A, Lay AC. Podocyte bioenergetics in the development of diabetic nephropathy: the role of mitochondria. Endocrinology. 2022;163(1):163.
8. Han X, Wang J, Li R, Huang M, Yue G, Guan L, et al. Placental mesenchymal stem cells alleviate podocyte injury in diabetic kidney disease by modulating mitophagy via the SIRT1-PGC-1alpha-TFAM pathway. Int J Mol Sci. 2023;24(5):4696.
9. Zheng T, Wang HY, Chen Y, Chen X, Wu ZL, Hu QY, et al. Src activation aggravates podocyte injury in diabetic nephropathy via suppression of FUNDC1-mediated mitophagy. Front Pharmacol. 2022;13: 897046.
10. Heineman BD, Liu X, Wu GY. Targeted mitochondrial delivery to hepatocytes: a review. J Clin Transl Hepatol. 2022;10(2):321–8.
11. Li X, Ruan T, Wang S, Sun X, Liu C, Peng Y, et al. Mitochondria at the crossroads of cholestatic liver injury: targeting novel therapeutic avenues. J Clin Transl Hepatol. 2024;12(9):792–801.
12. Clare K, Dillon JF, Brennan PN. Reactive oxygen species and oxidative stress in the pathogenesis of MAFLD. J Clin Transl Hepatol. 2022;10(5):939–46.
13. Liu Y, Zhang J, Wang Y, Zeng X. Apelin involved in progression of diabetic nephropathy by inhibiting autophagy in podocytes. Cell Death Dis. 2017;8(8): e3006.
14. Liu C, Li S, Ji S, Zhang J, Zheng F, Guan Y, et al. Proximal tubular Bmal1 protects against chronic kidney injury and renal fibrosis by maintaining of cellular metabolic homeostasis. Biochim Biophys Acta. 2023;1869(1): 166572.
15. Tokonami N, Mordasini D, Pradervand S, Centeno G, Jouffe C, Maillard M, et al. Local renal circadian clocks control fluid-electrolyte homeostasis and BP. J Am Soc Nephrol. 2014;25(7):1430–9.
16. Nikolaeva S, Ansermet C, Centeno G, Pradervand S, Bize V, Mordasini D, et al. Nephron-specific deletion of circadian clock gene Bmal1 alters the

plasma and renal metabolome and impairs drug disposition. J Am Soc Nephrol. 2016;27(10):2997–3004.
17. Meng X, Tan J, Li M, Song S, Miao Y, Zhang Q. Sirt1: role under the condition of ischemia/hypoxia. Cell Mol Neurobiol. 2017;37(1):17–28.
18. Halling JF, Pilegaard H. PGC-1α-mediated regulation of mitochondrial function and physiological implications. Appl Physiol Nutr Metab. 2020;45(9):927–36.
19. Qiu Z, Ming H, Zhang Y, Yu Y, Lei S, Xia ZY. The protective role of Bmal1-regulated autophagy mediated by HDAC3/SIRT1 pathway in myocardial ischemia/reperfusion injury of diabetic rats. Cardiovasc Drugs Ther. 2022;36(2):229–43.
20. Tang W, Guo R, Hu C, Yang Y, Yang D, Chen X, et al. BMAL1 alleviates myocardial damage in sepsis by activating SIRT1 signaling and promoting mitochondrial autophagy. Int Immunopharmacol. 2024;133: 112111.
21. Yang W, Kang X, Liu J, Li H, Ma Z, Jin X, et al. Clock gene Bmal1 modulates human cartilage gene expression by crosstalk with Sirt1. Endocrinology. 2016;157(8):3096–107.
22. Zhang P, Fang J, Zhang J, Ding S, Gan D. Curcumin inhibited podocyte cell apoptosis and accelerated cell autophagy in diabetic nephropathy via regulating beclin1/UVRAG/Bcl2. Diabetes Metab Syndr Obes. 2020;13:641–52.
23. Sindhuja S, Sivaperuman A, Nalini CN. A review on PCR and POC-PCR – a boon in the diagnosis of covid 19. Curr Pharm Anal. 2022;18:745.
24. Weil EJ, Lemley KV, Mason CC, Yee B, Jones LI, Blouch K, et al. Podocyte detachment and reduced glomerular capillary endothelial fenestration promote kidney disease in type 2 diabetic nephropathy. Kidney Int. 2012;82(9):1010–7.
25. Bhargava P, Schnellmann RG. Mitochondrial energetics in the kidney. Nat Rev Nephrol. 2017;13(10):629–46.
26. Ji H, Zhao Y, Ma X, Wu L, Guo F, Huang F, et al. Upregulation of UHRF1 promotes PINK1-mediated mitophagy to alleviates ferroptosis in diabetic nephropathy. Inflammation. 2024;47(2):718–32.
27. Hartleben B, Gödel M, Meyer-Schwesinger C, Liu S, Ulrich T, Köbler S, et al. Autophagy influences glomerular disease susceptibility and maintains podocyte homeostasis in aging mice. J Clin Invest. 2010;120(4):1084–96.
28. Zhang D, Pollock DM. Circadian regulation of kidney function: finding a role for Bmal1. Am J Physiol Renal Physiol. 2018;314(5):F675–8.
29. Liu H, Wang W, Weng X, Chen H, Chen Z, Du Y, et al. The H3K9 histone methyltransferase G9a modulates renal ischemia reperfusion injury by targeting Sirt1. Free Radical Biol Med. 2021;172:123–35.
30. Menzies KJ, Hood DA. The role of SirT1 in muscle mitochondrial turnover. Mitochondrion. 2012;12(1):5–13.
31. Ding M, Feng N, Tang D, Feng J, Li Z, Jia M, et al. Melatonin prevents Drp1-mediated mitochondrial fission in diabetic hearts through SIRT1-PGC1α pathway. J Pineal Res. 2018;65(2): e12491.
32. Rius-Pérez S, Torres-Cuevas I, Millán I, Ortega ÁL, Pérez S. PGC-1α, inflammation, and oxidative stress: an integrative view in metabolism. Oxid Med Cell Longev. 2020;2020:1452696.
33. Ploumi C, Daskalaki I, Tavernarakis N. Mitochondrial biogenesis and clearance: a balancing act. FEBS J. 2017;284(2):183–95.
34. Palikaras K, Tavernarakis N. Mitochondrial homeostasis: the interplay between mitophagy and mitochondrial biogenesis. Exp Gerontol. 2014;56:182–8.

Publisher's Note